THE MECHANICAL PROPERTIES OF RAPID-HARDENED MULTI-COMPONENT ALLOYS ON TiNi BASIS NEAR CRYSTALLIZATION TEMPERATURE

M.B. BABANLI
Azerbaijan Technical University
H. Javid ave.,25, Baku, Azerbaijan

The systematic investigations of mechanical properties of rapid-hardened tapes of multi-component alloys on TiNi basis of two types: *A* and *B* are carried out. The first lot is *A*, where only Cu in the samples $Ti_{32}Hf_{18}Ni_{50-x}Cu_x$ (where x=0; 5; 15; 25; 35; 45 at.%) varies in the composition. The second lot is *B* (Ti, Hf, Zr) (Ni, Cu, Co, Ag, Pd), where the doping elements Hf, Zr, Pd, Ag, Co, Cu vary on NiTi basis. All alloys with amorphous, mixed amorphous and crystalline phases demonstrate the elastic behavior before destruction moment in the "after obtaining" state.

Introduction.

The technique modern development requires more and more new perfect materials. The unit loads, the exploitation temperature conditions and medium aggressiveness increase. The question about the decrease of construction weight, durability increase, reliability and stability of material properties remains very acute. Meanwhile, the resource of property increase of standard alloys practically settles itself. That's why nowadays the materials with heterogeneous and metastable structures are widely used in increasing frequency.

The structure and phase composition of obtained material can strongly differ from equilibrium ones at alloy solidification (both metallic and non-metallic) with cooling rates on the level $10^5 - 10^6$ K/c. The more typical effects are: the formation of new metastable phases (amorphous and crystal), the widening of solubility limits of doping elements, the decrease of granule and inclusion dimensions. In spite of many experimental and theoretical works, there is no total clearness about formation of rapid-hardened material structure up to now. The two questions are very important from practical point of view: how to obtain the material in the amorphous state (to suppress the crystallization) and how to carry out diffusionless crystallization.

The systematic investigation of structural changes of rapid-hardened straps of multi-component alloys on TiNi base in our previous works [1-5] had carried out by the methods of *X*-ray analysis, translucent microscopy and calorimetry.

The systematic investigations of mechanical properties of rapid-hardened tapes of multi-component alloys on TiNi base at different temperatures and especially the interest results by our opinion are obtained near the temperatures T_g and T_x are carried out in the present work.

The material choice and experiment technique. The choice of chemical composition for multi-component alloys with shape memory effect on TiNi base, which further will be obtained by super rapid hardening from the melt, is based on two principles. Firstly, the chemical composition should be related to amorphization at super rapid hardening from the melt; secondly, the alloy should have the martensate transformations in the massive state (before super rapid hardening from the melt).

The multi-component alloys on TiNi base of two plots: *A* and *B* are chosen for the investigation. First plot is *A*, where only Cu in the composition varies in the samples $Ti_{32}Hf_{18}Ni_{50-x}Cu_x$ (where x=0; 5; 15; 25; 35; 45 at%). The second plot is *B* (Ti, Hf, Zr)(Ni, Cu, Co, Ag, Pd), where the doping elements Hf, Zr, Pd, Ag, Co, Cu vary on TiNi base.

The rapid-hardened tapes (foils) obtained from "master" alloys, the solidification from the melt; by Planar Flow Jasting are investigated in our work. In this method the distance between disk and melt is constant in the quartz crucible (less than 1 mm, in our case the distance is from 0,15 up to 0,2mm). The melt from the crucible proceeds from crack by the width 0,3-0,35mm and thickening 7-10mm, that allows obtaining the more wide tapes, than in our previous works. The cylindrical pieces of alloy (from 0,5 up to 15g) are stirred in quartz tube with the melt and are heated by inductive method. The melt temperature is controlled by pyrometer. The temperature, at which the gutter began, is 50-150K, that is higher than liquidus temperature and depends on the melt viscosity. The melt is put on the disk under argon pressure 0,2MPa. The disk by diameter 200 mm is produced from cuprum alloy Cu(Co – Be). The disk spinning rate is from 5 up to 30 m/c, the gas pressure is 0,2 MPa in the helium atmosphere [1].

The choice of the given alloys, obtained by super rapid hardening from the melt allows obtaining the different structural states after hardening at once (in initial state), and also investigating the evolution of structure and mechanical properties at the heating, the characteristics of martensate transformations after crystallization.

The nominal chemical composition of investigated rapid-hardened tapes of *A* plot ((Ti, Hf) (Ni, Cu) and *B* plot (Ti, Hf, Zr) (Ni, Cu, Co, Ag, Pd), the melt temperature at the output *Tq* and the width of obtained foils d are given in the tables 1 and 2.

Table 1.

The nominal chemical composition of rapid-hardened foils of A plot (T, Hf) (Ni, Cu), the melting point at the output *Tq* and foil width *d*.

Alloy	Nominal chemical composition (at%)				*Tq* (°C)	*d* (mcm)
	Ti	Hf	Ni	Cu		
A0	32	18	50	-	1380	30
A1	32	18	45	5	1296	30
A2	32	18	35	15	1285	30
A3	32	18	25	25	1300	30
A4	32	18	15	35	1200	30
A5	32	18	5	45	1100	30

The differential scanning calorimeter (DSC) Mettler DSC 30 and Mettler DSC 822e is used for the investigation of thermodynamic properties. These installations allow carrying

out the investigations in temperature interval from -150°C up to 700°C with heating rate 10-100K/c and cooling rate 10-20K/c. The sample mass from 5 up to 10mg, the bays type, in which the samples are situated: aluminum or platinum ones.

Table 2.
The nominal chemical composition of rapid hardened foils of *B* plot (Ti, Hf, Zr)(Ni, Cu, Co, Ag, Pd), melt temperature at the output *Tq* and foil width *d*.

Alloy	Nominal chemical composition (at%)					*Tq* (°C)	*d* (mcm)
	Ti	Hf ore Zr	Ni	Cu	others		
B0	50	-	25	25	-	1280	
B3	47	Hf-3	23	24.5	Pd-2 Ag-0.5	1320	30
B5	48	Zr-2	23	23	Pd-2 Ag-2	1280	30
B8	48	Zr-7	18	23	Pd-2 Ag-2	1320	30
B12	48	Zr-7	18	25	Co-2	1280	30
B20	27	Hf-18	50	5	-	1300	30
B21	27	Hf-18	40	15	-	1230	40
B22	27	Zr-18	50	5	-	1250	30
B23	27	Zr-18	40	15	-	1230	40
B24	40	Hf-15	8	37	-	1100	20
B25	40	Hf-15	3	42	-	1100	20

The machine for mechanical tests Test GmbH is used for investigation of mechanical properties of rapid-hardened foils. The given machine is additionally supplied by heating camera, that allows to us carrying out the investigations in the wide temperature interval from 20 up to 700°C with regulation of temperature and heating rate.

The investigated samples have the following dimensions: the length is ~40mm, width is 6-8, 4mm, the work part is 10mm.

The experiments are carried out on the following schemes:

1. The main mechanical properties (strength limit σ_f, Yung module *E*, maximum deformation before destruction ε_{max}) and deformation behavior of rapid-hardened tapes in the state "after obtaining" at room temperature (without heating). The mode "hard" machine is used. The program assigns the rate to the deformation ε', which varies in the range $8{,}3*10^{-1}$–$8{,}3*10^{-4}$ c^{-1}.

2. The investigations of the main mechanical properties and deformation behavior of rapid-hardened tapes in the state "after obtaining" at high temperatures (higher than room one) are carried out on the same scheme, described in the item 1, the only difference consists in the fact, that investigation temperature is varied in the interval from 20 up to 700°C (but each following experiment is carried out at constant given temperature).

3. The investigations of deformation behavior of rapid-hardened foils in the state "after obtaining" at the heating, i.e. investigation of superplasticity effect on the scheme "constant dynamic loading": the "hard" machine mode is used. The sample is loaded up to the definite value (200-500MPa), further, the machine supports the given loading value; moreover, deformation rate is constant. After it, the sample is heated with the rate 100K/min and the deformation graphical charts "loading – deformation" and "deformation – temperature" are written. The data about deformation behavior of amorphous and amorphous-crystal samples in temperature interval T_g-T_x can be obtained with the help of this mode, which the mode of "hard" machine.

The results and their discussion. The curves "voltage – deformation" for the investigated alloys are presented on the fig.1. The main mechanical properties for multi-component foils on TiNi base in the initial state ("after obtaining") are given on the table 3. All samples, which are in the initially amorphous state, demonstrate σ_f=740÷1110 MPa (for A plot), 810÷1410 MPa (for B plot), *E*=15÷39 MPa (for both plots); ε_{max}=2,4-7,3% (for both plots).

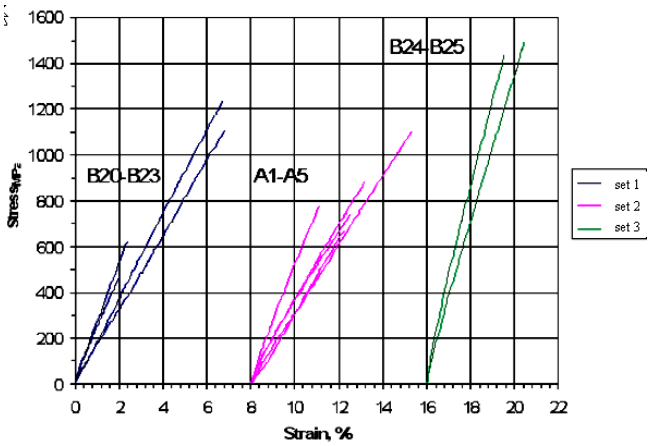

Fig.1. The curve "voltage – deformation" for the multi-component foils on TiNi base in the initial state ("after obtaining") at *T*=20°C.

The samples with mixed (amorphous-crystalline) structure show the values: σ_f=480÷1080 MPa; ε_{max}=2–6,8% and *E*=16÷28 MPa (for both plots). All alloys of plots *A* and *B* with totally amorphous structure demonstrate the higher strength limit, than alloys with mixed structures.

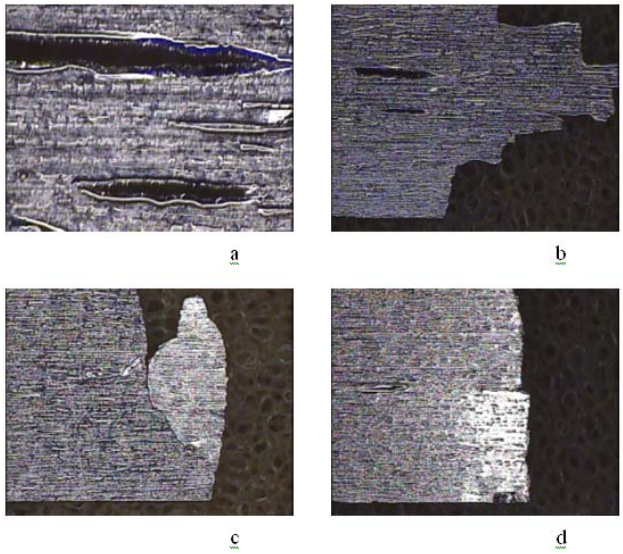

Fig.2. The surface of rapid-hardened foils after mechanical tests at *T*= 20°C, obtained with the help of light microscopy; a is *A2* alloy after mechanical tests at *T*=20°C (pore development); b are "icicles" of *A2* alloy; c are cracks of *B5* alloy; d are perpendicular directions to the axis of applied loading of *B12* alloy.

Table 3.

The main mechanical properties for multi-component foils on TiNi basis in the initial state ("after obtaining") at T=20°C: σ_f is breaking point; E is Yung module; ε_{max} is deformation before destruction.

Alloy, nom. ch. comp., at.%	Relations *A:B*	Structure "after obtaining"	σ_f, MPa	E, GPa	ε_{max}, %
A1-Ti32Hf18Ni45Cu5	50:50	Amorph.+Cr.	680	16,6	4,2
A2-Ti32Hf18Ni35Cu15	50:50	Amorph.	740	15,4	4,6
A3-Ti32Hf18Ni25Cu25	50:50	Amorph.	1110	15,0	7,3
A4-Ti32Hf18Ni15Cu35	50:50	Amorph.	890	16,4	5,2
A5-Ti32Hf18Ni5Cu45	50:50	Amorph.	790	22,3	3,1
B20-Ti27Hf18Ni50Cu5	45:55	Amorph.+Cr.	480	22,1	2,0
B21-Ti27Hf18Ni40Cu15	45:55	Amorph.+Cr.	1120	16,2	6,8
B22-Ti27Zr18Ni50Cu5	45:55	Amorph.	630	25,6	2,4
B23-Ti27Zr18Ni40Cu15	45:55	Amorph.	1240	18,6	6,8
B24-Ti40Hf15Ni8Cu37	55:45	Amorph.	1460	38,7	3,6
B25-Ti40Hf15Ni3Cu42	55:45	Amorph.	1510	32,5	4,5
B3-Ti47Hf3Ni23Pd2Cu24,5Ag0,5	50:50	Amorph.+Cr.	1200	19,6	6,1
B5-Ti48Zr2Ni23Pd2Cu23Ag2	50:50	Amorph.+Cr.	810	19,0	4,2
B8-Ti48Zr7Ni18Pd2Cu23Ag2	55:45	Amorph.	1410	21,0	6,9
B12-Ti48Zr7Ni18Cu25Co2	55:45	Amorph.+Cr.	980	18,9	5,1

The inclination of alloy chemical composition from relation *A:B*=50:50 leads to the increase of alloy durability level. This result well agrees with liquidus point: the highest liquidus temperature is fixed for the relation 50:50 and decreases at the inclination from this relation. The liqudus temperature influences on temperature interval of co-existence of liquid and crystalline phases, atom diffusion activity, containing in the composition, cooling rate, that exchanges the alloy structure in the initial state ("after obtaining") and their mechanical properties. The foil surface in the process of mechanical influences is investigated by optical microscopy and scanning electron microscopy in order to establish the possible deformation mechanisms in the foils with different initial structures. The following surface peculiarities are fixed: 1) The pore development at loading of *A2* alloys, if they are present before deformation (fig.2, a); 2) The stairs, formed by the shift with orientation approximately 45° in the relation to axis of applied loading, if the destruction surface is practically perpendicular to loadings (fig.2, *A2* alloy); 3) The tracks, formed by the shift with orientation approximately 45° in the relation to loading axis (B5 alloy), if the destruction surface is practically perpendicular to loading axis for *B5* and *B12* alloys (fig.2).

The application of term "shift" in the materials with amorphous structure doesn't mean that the shift of one atom square in the relation to another one takes place, this is impossible in the materials with amorphous structure. For the given materials the term "shift" means the shift of one material part relatively another one (in mane cases at angle of 45^0 to axis of applied voltage).

The images of destruction surface on the fig.3, obtained with the help of scanning electron microscopy, show the presence of "branched" pattern in *B12* alloy samples at room temperature after expansion. It is well known, that the presence of this pattern is character peculiarity for the material destruction surface with amorphous structure: it forms in the result of the fact that whole information accumulated in shift thin bands [1].

The micropores appear in these tapes, they expand and fill the spaces along shift s and further the isolation of atomic distances takes place. Moreover, the "branched" pattern is observed on the surface. These data show that the destruction has viscous character at the loading; the behavior of shift tapes is similar to the behavior of thin viscous full sphere between two parallel plates, that isn't practically deformed with formation of "branched" pattern. This is specific feature for destruction of metals and alloys with amorphous structure.

The destruction mechanism, which shows the formation of so-called "liquid drops", is supposed by authors of work [6]. The authors of work [6] suppose the alloy decomposition mechanism with amorphous structure, the essence of which consists in the fact that the material in the local regions (shift tapes) is heated in the result of transformation adiabatic process by accumulated deformation energy into warmth. This process leads to alloy local crystallization with amorphous structure (formations of "liquid drops") and to the destruction in the result it. The microstructure surface analysis in destruction region doesn't reveal the presence of "liquid drops", i.e. the supposed destruction mechanism isn't proved on our alloys neither with the help of optical electron microscope, nor with the help of scanning electron one. On the other hand, the series of experiments and calculations is carried out for the possibility designation of this destruction mechanism.

The information about deformation rate on the basis of mechanical properties for model alloys *B23* and *B25* can be critic one for the possible decomposition mechanism. Both alloys have the initial amorphous structure. The deformation rate for these alloys in the wide interval 0,5-500 nm/min doesn't practically influence on strength limit and Yung module. The elastic behavior of all alloys up to decomposition moment is the one from the reasons of the given result, and another one consists in the fact that foils have the big external surface and small width, that's why the warmth, which possible forms at the deformation, is transformed very quickly into environment.

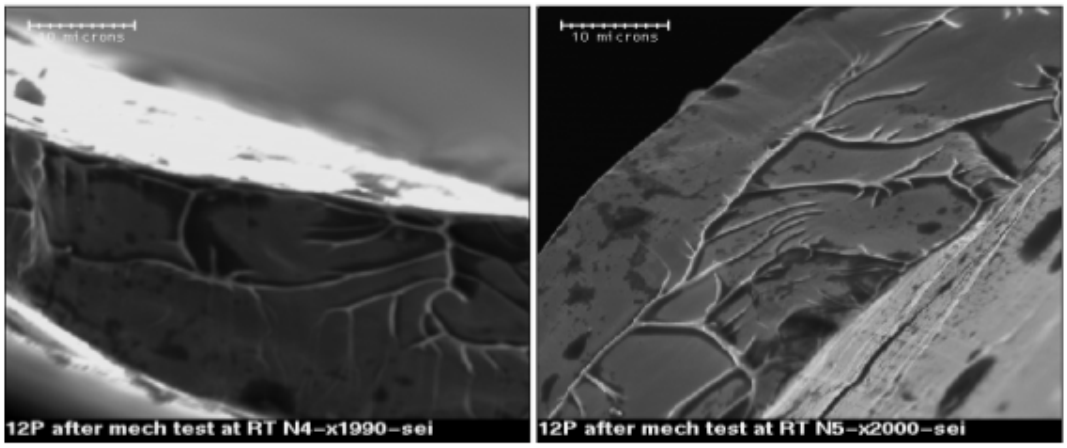

Fig.3. The destruction surfaces (scanning microscopy) of *B12* alloy after mechanical tests at T=20°C.

It is necessary to note the some difficulties, which appear at the definition of mechanical properties of rapid-hardened foils. These problems are connected with the presence of technological defects in the material, such as: the pores and irregularity to foil width. Moreover, this irregularity is fixed in two directions of cut: lengthwise and transversally foil length and has the form "wave" surface. Before testing the samples are investigated with the help of optical microscope, and also the measurement statistics is constructed in order to decrease the influence of these defects on the measurement results.

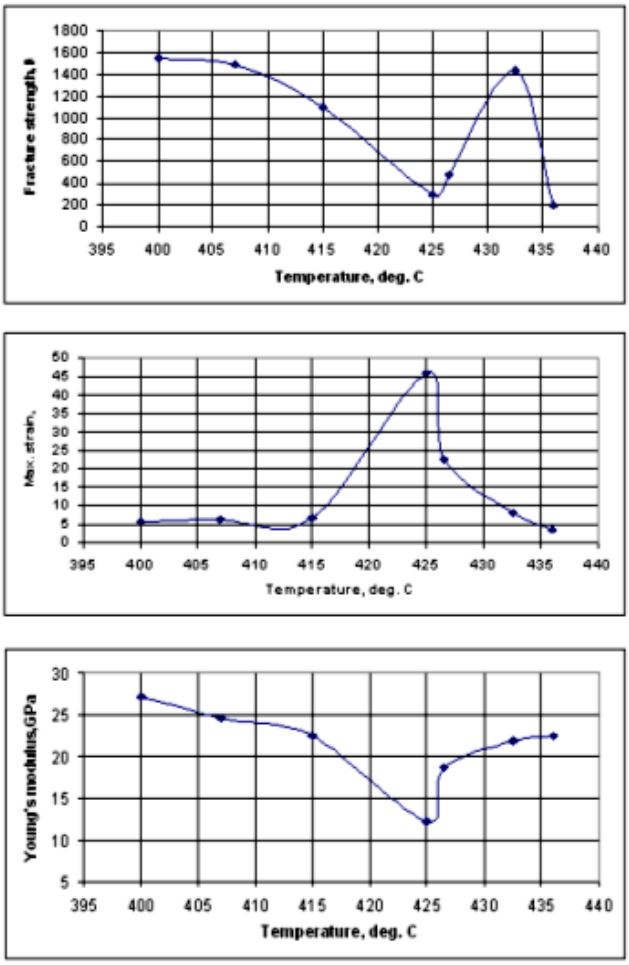

Fig.4. The dependence of the main mechanical properties (σ_f, E and ε_{max}) on the temperature of *B24* alloy.

The alloys with different structural states "after obtaining" are investigated for the study of deformation behavior at temperatures, which are higher, than room ones. The dependencies of main mechanical dependencies (durability limit σ_f, Yung module E, maximum deformation up to destruction ε_{max}) on the temperature for *B24* alloy, strain rate ε=5mm/min are presented on the fig.4.

The alloy deformation with amorphous structure can be conditionally divided into two types: homogeneous and nonhomogeneous [7-13]. The deformation type changes from nonhomogeneous up to homogeneous one at some critical temperature T_c with temperature increase. The critical temperature T_c depends on alloy strain rate [8,9]. The critical temperature for *B24* alloy is ~415°C, the strength strongly decreases at temperature increase higher than T_c, increasing with temperature increase.

The maximum deformation before deconstruction increases. The peak appears at the deformation of homogeneous alloys of amorphous types with temperature increase, and further, decreases at crystallization process leaking. The increase of maximum deformation up to destruction well agrees with temperature dependence of alloy viscosity [8, 14-18].

Yung module decreases with at temperature increase, forming the minimum and after it increases at crystallization process leaking. This result shows, that force of interatomic interaction becomes less in T_g region. This result hasn't the clear physical explanation yet [7]. The alloy durability level decreases at more high temperatures, which are higher than T_g at formation of crystalline granules in the amorphous matrix. The deformation scheme: "constant dynamic loading" is worked for the study of deformation behavior and high durability effect in rapid-hardened foils. The high plasticity is the effect, which is character for amorphous structure at glass-transition temperatures T_g. The dependencies "deformation – voltage" and "deformation – temperature", obtained in the experiment result on the scheme "constant dynamic loading" for *A1*, *A2*, *3P*, *B12*, *B23* alloys are presented on the fig.5. The samples demonstrate the different maximum deformation before destruction ε_{max}, for example, for *A1* alloy is 19%, for *A2* alloy is 62%. These results show that alloys with mixed structure (amorphous-crystalline) also have the high plasticity effect and maximum deformation depends on volume part of crystalline phase in amorphous matrix.

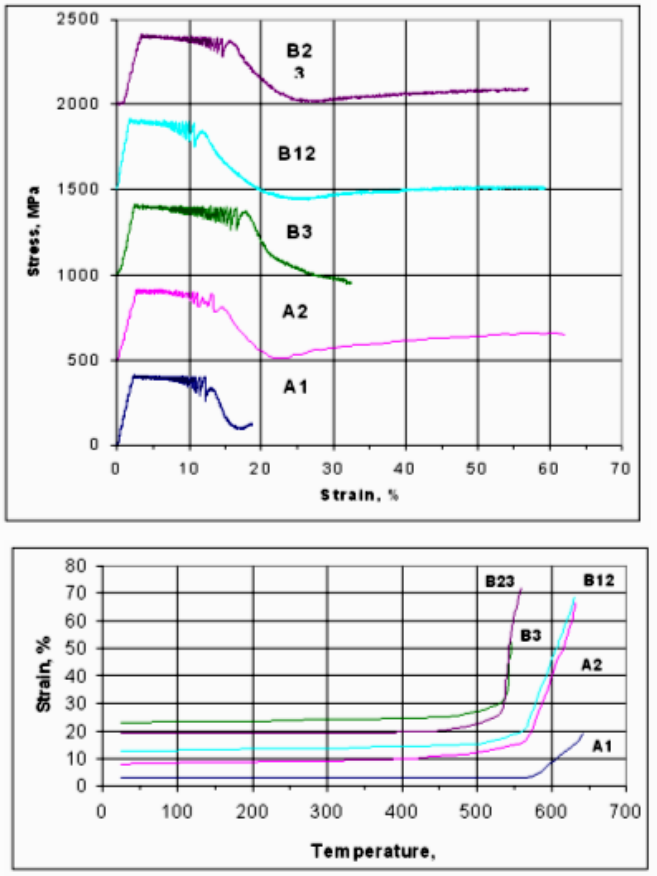

Fig.5. The dependencies "deformation - voltage" and "deformation – temperature" for alloys *A1*, *A2*, *B3*, *B12* and *B23*, obtained in the result of experiments on the scheme "constant dynamic loading".

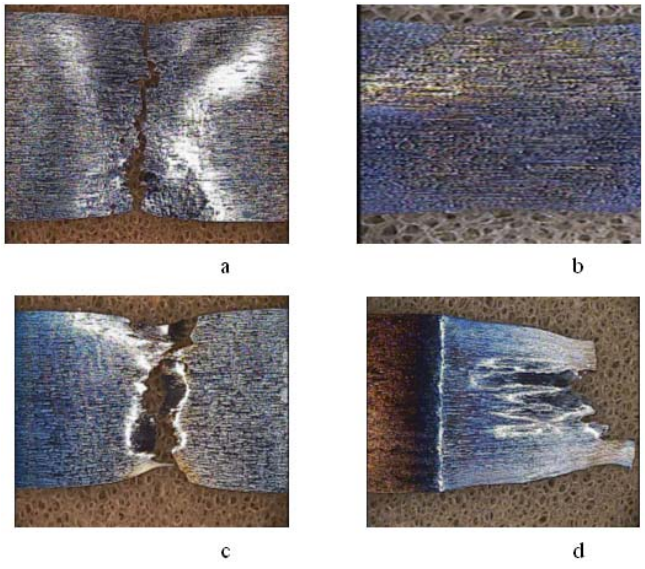

Fig.6. The foil surfaces (optical microscope) after experiment on the scheme "constant dynamic loading" l a is *A1* alloy; b is *A2* alloy; c is *B3* alloy; d is *B12* alloy.

The surface images of rapid-hardened foils of *A1*, *A2*, *3P*, *B12* alloys after investigation on the scheme "constant dynamic loading" are presented on the fig.6. These images are obtained with the help of optical microscope. All samples have the constrictions in the middle work part that is the result of material viscous deformation.

The transition of deformation nonhomogeneous type up to homogeneous one is accompanied by the fact that the maximum, so-called "tooth" (fig.7) appears on curves "voltage – deformation". The "tooth" height $\Delta\sigma$ is the difference between maximum voltage σ_p and concealed voltage σ_s, which decreases at temperature increase and strain rate decrease [7]. It is impossible to explain the "tooth" phenomenon with the help of dislocation theory (as dislocations are absent in amorphous structure) [7], and it can be result of viscous-elastic behavior of amorphous alloys, where the role of viscous concealed voltage becomes essential at more high temperatures and less strain rates in the relation to elastic behavior (at room temperature).

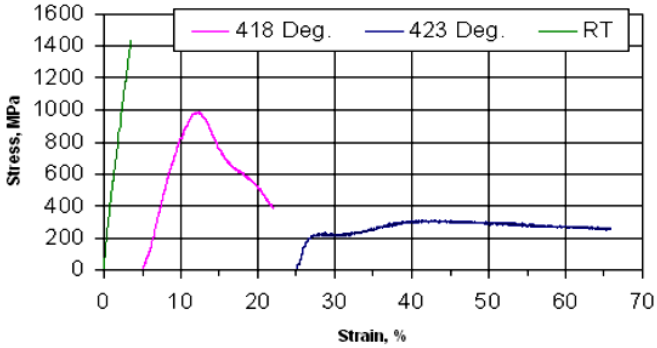

Fig.7. The deformation behavior of *B24* alloy in the dependence on the temperature ("voltage – deformation").

The influence of strain rate on maximum deformation up to *B23* alloy destruction is presented on the fig.5. The maximum deformation before destruction ε_{max} increases, forming the peak at critical strain rate ε_c^1 and after it decreases at increase of strain rate.

The influence of strain rate on the value of concealed voltage σ_{flow} and viscosity η for *B23* alloy are presented on the fig.8. The material viscosity is calculated with the help of the formula (1) [8]:

$$\eta = \sigma_{flow} / 3\varepsilon' . \qquad (1)$$

The viscosity stays practically constant value for strain rate, but doesn't exceed the critical ε_c^1 and decreases at deformation rates, which exceeds the critical one. The value of critical deformation rate ε_c^1 is responsible for cut point of dependencies $\eta=\Phi(\varepsilon')$ and divides the deformation mode into low- and high-speed ones.

The concealed voltage σ_{flow} linearly increases with increase of deformation rate and forms "plateau" at deformation rate, which exceeds the critical one. The critical deformation rate at constant temperature is the one of important deformation parameters, as it shows the maximum deformation before destruction, which is possible to achieve. The amorphous alloy demonstrates Newton type of concealed voltage at low-speed deformation mode and non-Newton one at high-speed deformation mode.

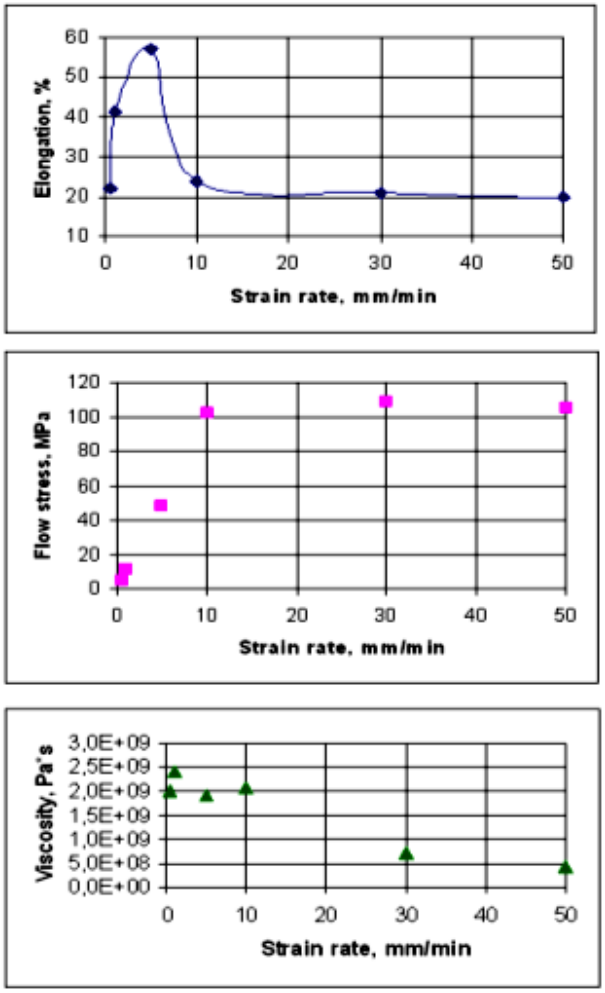

Fig.8. The dependencies of maximum deformation, voltage and viscosity of *B23* alloy before destruction on the strain rate.

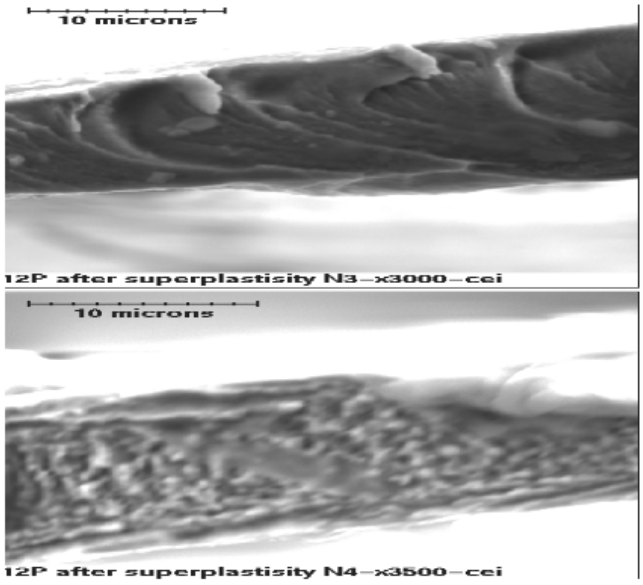

Fig.9. The destruction surface of *B12* alloy after the test on the scheme "constant dynamic loading".

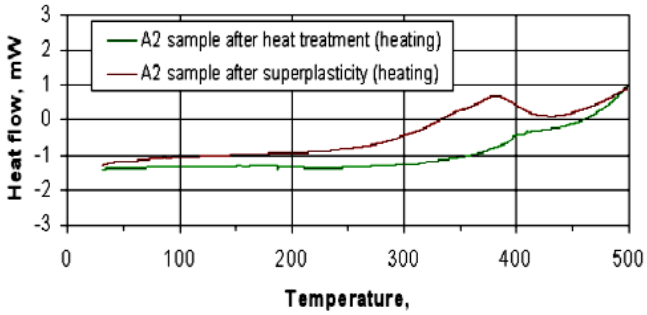

Fig.10. The calorimetric curves of rapid-hardened foils of *A2* alloy after the superplasticity effect and thermal working at 630°C during 10 minutes in "free state" (without loading).

The destruction surface image of *B12* alloy sample after high plasticity effect is presented on the fig.9. As it is seen from the fig.9., the microstructure of destruction surface isn't homogeneous one: the regions with intergranular destruction type and regions with "sudino-like" type, which is character for destruction of amorphous phase, are presented. The some volume part of material stays amorphous after high plasticity effect. The calorimetric curves for A2 and B3 alloys are presented on the fig.10 and 11, correspondingly. The calorimetric curves for foils of A2, which have the different pre-histories after high plasticity and thermal working in "free" state (without loading), at similar thermal conditions 630 ^{0}C during 10 minutes, are shown on the fig.10. The following result is obtained: the some alloy part stays amorphous after high plasticity effect after thermal working in "free" state. The analogous result is obtained for B3 alloy.

Conclusion. Thus, A:B relation inclinations from 50:50 up to 55:45 and 45:55 in alloy chemical composition in many cases lead to appearance of foil strength level in the state "after obtaining". This result well agrees with liquidus temperature variation, which is fixed exactly for relation "A:B" 50:50 and decreases at the inclination from this relation. It is established, that doping element variation: the introduction of Zr instead of Hf, changes the structure in the state "after obtaining" from mixed amorphous-crystalline phases to totally amorphous one. As a result, the alloys of TiZrNiCu system demonstrate the highest durability level, than alloys of TiHfNiCu system.

All alloys with amorphous and mixed crystalline phases in the state "after obtaining" demonstrate the elastic behavior up to the destruction moment. It is shown, that both normal and sufficient voltages influence on the destruction of rapid-hardened foils (the destructions have viscous nature with formation of "sudino-like" pattern, which is typical for materials with amorphous structure).

The strain rate in wide interval 0,5-500 mm/min doesn't influence on strength limit and Yung module for the alloys of amorphous and mixed amorphous-crystalline structures in the state "after obtaining".

The rapid-hardened foils on TiNi basis with amorphous and mixed (amorphous-crystalline) structures demonstrate high plasticity effect near glass-transition temperatures T_g.

[1] *M.B. Babanlı*. Bıstrozakalennıye splavı. Baku: «ELM», 2004, 441s. (in Russian).

[2] *M.B. Babanlı*. Zavisimost vozniknoveniya amorfnoqo sostoyaniya ot koncentracii medi i skorosti zakalki iz rasplava v splava TiNiCu. Sb. statey Fiziko-xim. analiz i neorqan. materialovedeniye, Baku, 1997, s.184-187. (in Russian).

[3] *M.B. Babanlı, V. Kolomıcev, A. Sezonenko*. Fazovıye i strukturnıye sostoyaniya voznikayushiye v splavakh TiNiCu. Sb. statey Fiziko-khim. analiz i neorqan. materialovedeniye, Baku, 2002, s.240-246. (in Russian).

[4] *V. Kolomytsev, M. Babanly, R. Musienko, A. Sezonenko, P. Ochin, A. Dezellus, P. Plaindoux, R. Portier, P. Vermaut*. The transformation kinetics of the multikomponent TINI based melt spun ribbons from the amorpous to nanocrystallic state .Metallofizika I noveysie texnoloqii Kiev, 2001, v..23, p. 124 – 137.

[5] *V. Kolomytsev, M. Babanly, R. Musienko, A. Sezonenko*. Structure and functional properties of some multicomponent TiNi- dased Shape Memory melt-spun ribbons. Sb. statey «Fundamentalniye i prikladniye problemi fiziki» g. Ternopol (Ukraina), 2000, p.159-160.

[6] *L.Q. Xing, C. Bertrand.,J.P. Dallas, M. Cornet*. Nanocrystal evolution in bulk amorphous $Zr_{57}Cu_{20}Al_{10}Ni_8Ti_5$ alloys and ist mechanical properties. Materials Science and Engineering, 1998, A241, p.216 - 225 .

[7] *R. Bush*. JOM, 2000, 52(7), p.39 – 42.

[8] *H. Kato, Y. Kawamura, A. Inoue, H.S. Chen*. Appl. Phys. Lett., 1998, v.73, p.3665-3667.

[9] *Y. Kawamura, T. Shibata, A. Inone, T. Masumoto*. Appl. Phys. Lett., 1997, v.71 (6), p.779 – 781.

[10] *M.B. Babanlı, V.A. Lobodyuk*. Osobennosti perekhoda iz amorfnoqo v kristallicheskoye sostoyaniye v splavakh TiNiCu. Sbornik nauchnıkh trudov «Fiziko-khimicheskiy analiz i neorqanicheskoye materialovedeniye». Baku, 1996. s.109-112. (in Russian)

[11] *M.B. Babanli.* Texnoloqiya polucheniya mnoqokomponentnikh splavov $(Ti,Hf)_{50}(Ni,Cu)_{50}$ i $(TiHf,Zr)_{50}[(Ni,Co)(Cu,Ag)]_{50}$ /Sb. statey Fiziko-khim. analiz i neorqan. materialovedenie, Baku, 1999, s. 218-223

[12] *M.B. Babanly, V.A. Lobodyuk, N.M. Matveeva.* Proc. Conf. "Martensite-91", Kiev, 1992, pp. 338-341.

[13] *M.B. Babanly, V.A. Lobodyuk, N.M. Matveeva.* Izvestiya Academy of Sciences USSR, Metals 5 (1993) 171-177.

[14] M.B. Babanli. Splavi s effektom pamyati formi. Baku:«ELM»,2006, 280s.

[15] *M.B. Babanli, V. Kolomitsev, A. Sezonenko.* Osobennosti vliyaniya termomekhanicheskoy obrabotki na kharakteristiki martensitnoqo prevrasheniya v splavakh TiNiCu. Sb. statey Fiziko-khim. analiz i neorqan. materialovedenie, Baku, 2002, s.235-239

[16] *M.B. Babanli, V. Kolomitsev, A. Sezonenko.* Fazovie i strukturnie sostoyaniya voznikayushie v splavakh TiNiCu /Sb. statey Fiziko-khim. analiz i neorqan. materialovedenie, Baku, 2002, s.240-246.

[17] *M.B. Babanli, Z.E. Salimov.* Strukturnie izmeneniya v splavakh na osnove TiNi. Sb. nauch. tr. konfer. AzTU, Baku, 2001, s.217-219.

[18] *M.B. Babanli.* Nekotorie voprosi polucheniya amorfnikh i nanokristallicheskikh materialov. Sb. nauch. tr. konfer. AzTU, Baku, 2006, s.153-156.

[19] *M.B. Babanli.* Martensitnie prevrasheniya v splavakh TiNiZr //Uchenie zapiski AzTU, №4, 2004, s. 31-34.

M.B. Babanlı

İFRAT SÜRƏTLƏ TABLANDIRILMIŞ TiNi ƏSASLI ÇOXKOMPONENTLİ ƏRİNTİLƏRİNDƏ KRİSTALLAŞMA TEMPERATURU YAXINLIĞINDA MEXANİKİ XASSƏLƏR

İfrat sürətlə tablandırılmış TiNi əsaslı çoxkomponentli ərintilərin mexaniki xassələri iki seriyada sistemli şəkildə tədqiq edilmişdir: A və B. Birinci, A seriyada tərkibdə yalnız Cu $Ti_{32}Hf_{18}Ni_{50-x}Cu_x$ (x=0; 5; 15; 25; 35; 45 at. %)əvəz edilmişdir. İkinci V (Ti, Hf, Zr)(Ni, Cu, Co, Ag, Pd) seriyada isə NiTi sistemi tərkibində Hf, Zr, Pd, Ag, Co, Cu kimi leqirləyici elementlər dəyişdirilmişdir. Məlum olmuşdur ki, öyrənilmiş ərintilərdə «ilkin vəziyyətdə» amorf və amorf – kristallik quruluşa malik təbəqələr dağılmaya qədər elastiklik xassələri göstərir.

М.Б. Бабанлы

МЕХАНИЧЕСКИЕ СВОЙСТВА БЫСТРОЗАКАЛЕННЫХ МНОГОКОМПОНЕНТНЫХ СПЛАВОВ НА ОСНОВЕ Ti-Ni ВБЛИЗИ ТЕМПЕРАТУРЫ КРИСТАЛЛИЗАЦИИ

Проведены систематические исследования механических свойств быстрозакаленных лент многокомпонентных сплавов на основе TiNi двух серий: А и В. Первая серия А, где в составе варьируется только Cu в образцах $Ti_{32}Hf_{18}Ni_{50-x}Cu_x$ (де x=0; 5; 15; 25; 35; 45 ат. %). Вторая серия В (Ti, Hf, Zr)(Ni, Cu, Co, Ag, Pd), где варьировались легирующие элементы Hf, Zr, Pd, Ag, Co, Cu на базе NiTi. Все сплавы с аморфной и со смешанной аморфной и кристаллической фазами в состоянии «после получения» демонстрируют упругое поведение до момента разрушения.

Received: 12.09.07